Achillodynia – Radiological Imaging of Acute and Chronic Overuse Injuries of the Achilles Tendon

Achillodynie – Radiologische Bildgebung bei akuten und chronischen Überlastungsschäden der Achillessehne

Authors

R. Syha[1, 3], F. Springer[1, 3], D. Ketelsen[1], I. Ipach[2], U. Kramer[1], M. Horger[1], F. Schick[3], U. Grosse[1, 3]

Affiliations

[1] Diagnostic and Interventional Radiology, Eberhard-Karls-University, Tübingen
[2] Orthopaedic Surgery, University Hospital Tübingen
[3] Section on Experimental Radiology, Eberhard-Karls-University, Tübingen

Key words
- tendons
- MR imaging
- ultrasound

eingereicht 18.10.2012
akzeptiert 30.1.2013

Bibliography
DOI http://dx.doi.org/10.1055/s-0033-1335170
Published online: 25.7.2013
Fortschr Röntgenstr 2013; 185: 1041–1055 © Georg Thieme Verlag KG Stuttgart · New York · ISSN 1438-9029

Correspondence
Dr. Roland Syha
Diagnostic and Interventional Radiology, Eberhard-Karls-University
Hoppe-Seyler-Str. 3
Tübingen 72076
Tel.: ++ 49/70 71/2 98 04 95
Fax: ++ 49/70 71/29 46 38
roland.syha@gmx.net

Abstract

In the past decades the incidence of acute and chronic disorders of the Achilles tendon associated with sport-induced overuse has steadily increased. Besides acute complete or partial ruptures, achillodynia (Achilles tendon pain syndrome), which is often associated with tendon degeneration, represents the most challenging entity regarding clinical diagnostics and therapy. Therefore, the use of imaging techniques to differentiate tendon disorders and even characterize structure alterations is of growing interest. This review article discusses the potential of different imaging techniques with respect to the diagnosis of acute and chronic tendon disorders. In this context, the most commonly used imaging techniques are magnetic resonance imaging (MRI), B-mode ultrasound, and color-coded Doppler ultrasound (US). These modalities allow the detection of acute tendon ruptures and advanced chronic tendon disorders. However, the main disadvantages are still the low capabilities in the detection of early-stage degeneration and difficulties in the assessment of treatment responses during follow-up examinations. Furthermore, differentiation between chronic partial ruptures and degeneration remains challenging. The automatic contour detection and texture analysis may allow a more objective and quantitative interpretation, which might be helpful in the monitoring of tendon diseases during follow-up examinations. Other techniques to quantify tendon-specific MR properties, e. g. based on ultrashort echo time (UTE) sequences, also seem to have great potential with respect to the precise detection of degenerative tendon disorders and their differentiation at a very early stage.

Key Points:
- For radiological imaging in the clinical routine, different clinical presentations of acute or chronic overuse injuries of the Achilles tendon must be considered.
- In addition to qualitative morphological imaging criteria, supplementary quantitative criteria (planimetry/volumetry) of the Achilles tendon seem to be significant with respect to the differentiation between symptomatic and asymptomatic Achilles tendons.
- Other techniques to quantify tendon-specific MR properties, e. g. based on ultrashort echo time (UTE) sequences, seem to have great potential with respect to the precise detection of degenerative tendon disorders and their differentiation at a very early stage.

Citation Format:
- Syha R., Springer F., Ketelsen D. et al. Achillodynia – Radiological Imaging of Acute and Chronic Overuse Injuries of the Achilles Tendon. Fortschr Röntgenstr 2013; 185: 1041–1055

Zusammenfassung

Innerhalb der letzten Jahrzehnte hat die Inzidenz von akuten und chronischen Überlastungsschäden der Achillessehne stetig zugenommen. Die deutliche Zunahme in den letzten Dekaden lässt sich in erster Linie durch die erhöhte Freizeitaktivität in der Bevölkerung begründen. Neben den akuten Teil- oder Komplettrupturen der Achillessehne stellt die Achillodynie (Schmerzsyndrom der Achillessehne), welche häufig mit einer Sehnendegeneration einhergeht, eine Herausforderung für Diagnostik und Therapie dar. In diesem Zusammenhang hat der Einsatz von bildgeben-

den Verfahren zur Diagnostik und Charakterisierung sehnenspezifischer Veränderungen deutlich zugenommen. Im folgenden Übersichtsartikel werden die Möglichkeiten der aktuellen radiologischen Bildgebung bezüglich akuter und chronischer Überlastungsschäden der Achillessehne erörtert. Gängige bildgebende Verfahren stellen hier die Magnetresonanztomografie (MRT) sowie der B-Mode- und farbkodierte Ultraschall (US) dar. Hiermit lassen sich Komplettrupturen und fortgeschrittene degenerative Veränderungen gut detektieren. Schwächen haben die genannten Verfahren in der Diagnostik von Frühstadien der Tendinose und der Verlaufsbeurteilung unter Therapie. Die eindeutige Differenzierung zwischen chronischer Partialruptur und Tendinose kann eine Herausforderung darstellen. Neue automatisierte Konturerkennungsverfahren und Texturanalysen erlauben darüber hinaus auch eine quantitative Beurteilung der Achillessehne, was die objektive Beurteilung von Strukturänderungen im Krankheitsverlauf erleichtern und in seiner Qualität verbessern könnte. Weiterhin scheinen neue Methoden zur quantitativen, MR-tomografischen Charakterisierung des tendinösen Gewebes, z. B. mithilfe ultrakurzer Echozeiten (UTE), ein großes Potenzial zur frühzeitigen Erkennung und Verlaufsbeurteilung von degenerativen Veränderungen der Achillessehne zu haben.

Introduction

The incidence of acute and chronic pathologies of the Achilles tendon has increased considerably in the last decades. These diseases are often caused by overuse during sports, in particular sports involving running or a ball, or increased occupational strain [1]. Both external influencing factors (e. g. training conditions and equipment) as well as internal influencing factors (e. g. anatomical conditions or systemic diseases) can trigger the development of acute or chronic pathologies [2]. The use of imaging methods for such cases has increased. In addition to the primarily qualitative imaging methods typically used in the clinical routine (ultrasound, MRI), methods for quantitatively analyzing and characterizing pathologies of the Achilles tendon are increasingly being developed.

In the clinical routine consideration of the different clinical presentations of acute and chronic pathologies of the Achilles tendon that need to be differentiated in relation to morphology and location and require corresponding diagnostic methods is relevant for the selection of the suitable imaging method.

Imaging methods for evaluating the Achilles tendon

Due to their good soft tissue contrast, magnetic resonance imaging (MRI) and ultrasound have become the standard for diagnosing acute and chronic overuse injuries of the Achilles tendon [3, 4]. Conventional radiography and computed tomography (CT) play only a secondary role, for example, in the evaluation of possible bone involvement in an avulsion fracture at the calcaneus or in regard to the imaging of tendon calcification or bone spurs [5, 6]. Conventional radiography is also still valuable for diagnosing Haglund's exostosis [7].

Ultrasound

Due to its broad availability, good sensitivity for Achilles tendon pathologies, and comparably low costs, ultrasound is very frequently used as the primary method for diagnosing acute and chronic overuse injuries of the Achilles tendon [8]. However, the disadvantages of this method include examiner dependence and limited reproducibility [9]. To improve the detail resolution, high-frequency probes with a frequency of 7.5 MHz or higher are used [10, 11]. B-mode ultrasound is regularly used for visualizing anatomical structures and power Doppler is used for evaluating the vascularization of tendons and paratendinous tissue.

The patient is positioned in a prone position on the examination table. The ankle joint is positioned so that it protrudes past the rear edge of the examination table and should be held in the neutral-zero position. Transverse and longitudinal scans of the entire tendon are acquired. The longitudinal scans should always be at a 90 degree angle with respect to the greatest width of the Achilles tendon to prevent possible artificial hypoechogenicities in healthy tendons from being incorrectly evaluated as pathological [12]. In the longitudinal scan, healthy tendon tissue has a relatively homogeneous echo pattern with parallel linear echoes that show the fibrillar structure (**Fig. 1**) [10]. The boundaries (paratenon) are parallel to one another and can also be delimited. The important diagnostic parameter, the so-called true tendon thickness, should also be measured in this scan orientation [13, 14]. The standard value for healthy tendons is approx. 4 – 5 mm. The standard measurement is performed using a longitudinal scan in the center of the Achilles tendon approx. 2 – 4 cm from the bony insertion at the calcaneus [9, 14]. The smallest neovascularizations in the Achilles tendon can be visualized with power Doppler or color duplex sonography [15]. Power Doppler is superior to color duplex sonography with respect to diagnostic sensitivity in this regard [16].

MRI

The field strengths typically used in the clinical routine for the diagnosis of pathologies of the Achilles tendon are 1.5 T and 3 T. However, due to the increasing availability of high-field MRI units, MR examinations of the ankle joint and the surrounding tendons are increasingly being performed at a field strength of 3 T in recent years. The main advantage of the higher field strength is the almost linear increase of the signal-to-noise ratio (SNR) in relation to the field strength. The greater SNR compared to at 1.5 T can be used to either improve the spatial resolution or to reduce the measurement time with fewer averaging operations. Moreover, the frequency-specific fat suppression in the region of the extremities is faster and more robust at 3 T. This is mainly due to the greater chemical shift between fat and water (approx. 220 Hz at 1.5 T and approx. 440 Hz at 3 T) [17]. When comparing examination protocols for 1.5 T and 3 T, it must be taken into consideration that the T1 relaxation times at 3 T are approximately 15 – 20 % longer depending on the type of tissue while the T2 relaxation times at 3 T are only slightly shorter [18]. The main disadvantages of the higher field strength are increasing field inhomogeneity, more significant artifacts in the area of metal implants, and regional image shading caused by B1 field inhomogeneities [17]. The

Fig. 1 **a** The normal anatomy of the Achilles tendon in B-mode ultrasound images is presented in **a, b**. White arrows mark the boundaries of the Achilles tendon in the longitudinal view **a** while the proximal border of the calcaneal bone is marked by a white asterisk. The Achilles tendon shows a fibrillar homogenous echo pattern in longitudinal as well as in axial scans. **c**, **d** T2 weighted sagittal image without fat saturation and PD weighted image with fat saturation of the Achilles tendon at 3 T are presented. The healthy Achilles tendon appears dark. White arrows mark the boundaries of the Achilles tendon.

sequence	TE (ms)	TR (ms)	field strength (T)	FOV (mm)	resolution (mm³)	scan duration (min)
standard protocol at 1.5 T						
T1 TSE sagittal	21	500	1.5	220	0.5 × 0.5 × 3	3:21
T2 TSE axial	100	6640	1.5	160	0.8 × 0.8 × 3	3:58
PD TSE fs sagittal	29	4000	1.5	220	0.7 × 0.7 × 3	5:30
TIRM sagittal	32	4000	1.5	220	0.7 × 0.7 × 3	5:26
standard protocol at 3 T						
T1 TSE sagittal	12	600	3	220	0.3 × 0.3 × 3	3:20
T2 TSE axial	45	6000	3	160	0.3 × 0.3 × 3	3:26
PD TSE fs sagittal	54	3000	3	220	0.5 × 0.5 × 3	4:14
TIRM sagittal	43	3800	3	220	0.5 × 0.5 × 3	4:01

TE = echo time; TR = repetition time; FOV = field of view; TSE = turbo spin echo; PD = proton density; TIRM = turbo inversion magnitude; fs = fat saturation.

Table 1 Standard protocol for the examination of the Achilles tendon at 1.5 T and 3 T.

standard sequences at 1.5 T and 3 T are summarized in ▶ **Table 1**.

A healthy tendon has a low signal appearance due to its ordered structure and the limited intratendinous mobility of free water in T1, T2 and proton density (PD) weighting. It is uniformly narrow and extends for approx. 15 cm from the calcaneal insertion to the myotendinous junction. Fluid-sensitive sequences show the retrocalcaneal bursa in the form of a small hyperintense band of fluid on the ventral side above the calcaneal tuberosity. It is bordered apically and ventrally by the fat-isointense Kager's fat pad (▶ **Fig. 1**). Solitary focal intratendinous changes (usually point-shaped or longitudinally oriented) do not have any pathological value since they correspond to small connective tissue septa or small intratendinous vessels [19].

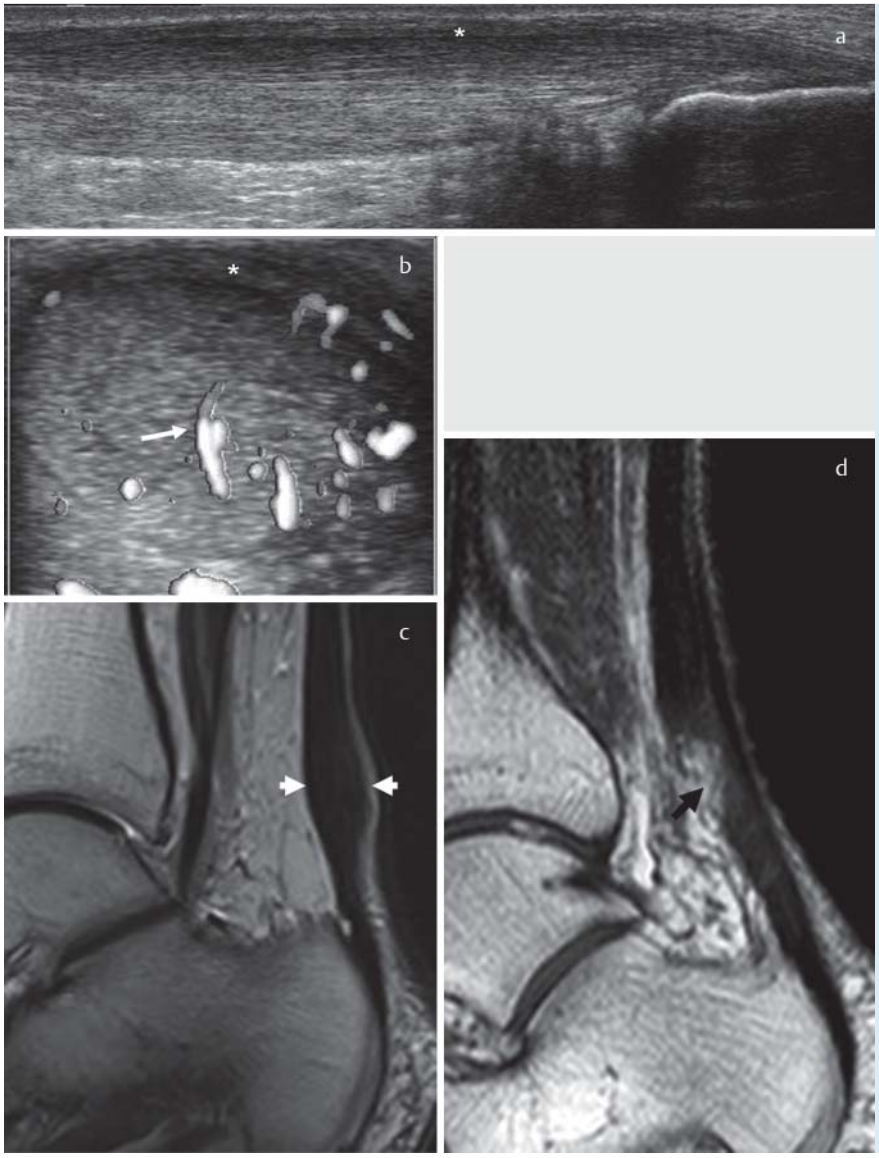

Fig. 2 **a** shows the typical spindle-shaped thickening of the Achilles tendon associated with degeneration, as well as focal hypoechoic areas in a 44-year-old patient. **b** shows intratendinous neovascularization (white arrow) associated with tendinopathy. An associated paratenonitis is present in terms of thickened tendinous boundary (marked by the white asterisk). **c** In comparison to ultrasound, a sagittal T2-weighted MR image also shows a spindle-shaped thickening and areas of signal alterations within the tendon (white arrows, **c**) in a 46-year-old patient with midportion tendinosis. **d** In contrast, a partial rupture of the Achilles tendon in a 77-year-old patient is shown in a sagittal T1-weighted MR image **d**. The fibrillar pattern of the Achilles tendon is interrupted as shown by the black arrow.

Pathologies of the Achilles tendon

The most important intratendinous and peritendinous changes visualized by imaging used in the clinical setting will first be discussed and then their significance in the general clinical and histological context will be explained in the following.

Intratendinous changes

Tendinosis

Tendinosis refers to a pathological change of the tendon due to degeneration. With approx. 60 % of cases, it is the most common form of tendinopathy of the Achilles tendon [1]. The often used term tendinitis is misleading since it suggests inflammation for which there is not histopathological evidence [20]. According to the current theory, both repetitive overuse as well as defective reparative processes on a cellular level can result in destruction of the fiber structure. Repetitive microtraumas (so-called tendinosis cycling) cause increasing fiber fatigue resulting in tendinosis [21]. In principle, there are four types of degeneration but they overlap and the individual types cannot always be precisely differentiated. Therefore, hypoxic, mucoid, lipomatous, and calcifying ossifying degeneration is described in the literature. While hypoxic and mucoid degeneration are often the result of chronic overuse and have the highest total prevalence, lipomatous degeneration is primarily the product of aging [22]. However, calcifications within the Achilles tendon as the result of an ongoing degeneration process are rather rare. According to histopathological studies, the different types of Achilles tendon degeneration are present in 90 % of symptomatic tendons and in up to 30 % of asymptomatic tendons [1, 20, 22].

In MRI as well as ultrasound, hypoxic degeneration is visualized as a spindle-shaped thickening of the Achilles tendon [10, 22, 23]. In the further course, the fibrillar echo pattern is lost and there is generalized hypoechogenicity of the tendon [10]. MRI sometimes shows slight signal enhancement in the T2 weighting [22, 24] (**Fig. 2**).

In MRI, mucoid degeneration is visualized with focal interstitial signal alterations and interruptions (hyperintensities in the T2 weighting and at times milder hyperintensity in the T1 weighting) [22]. Sonography frequently shows focal hypoechogenicities and microtears [10]. The Achilles ten-

Fig. 3 Different kinds of Achilles tendon ruptures are presented in **Fig. 3**. All images are sagittal PD-weighted with fat suppression. In **a** a complete tendon rupture (white arrow) in a 42-year-old patient in a typical location is shown (white arrow). The fibers show a clear dehiscence with accompanying edema and hematoma. In **b** a rare case of an insertional tendon rupture in a 51-year-old male patient is presented (white arrow). **c** shows a rupture within the myotendinous junction with hemorrhage and edema in a 43-year-old male patient (white arrow).

don thickness in the ventrodorsal diameter shows only a moderate increase to approx. 6 – 7 mm with the standard measurement being performed in the sagittal plane 2 – 4 cm from the calcaneal insertion under consideration of the abovementioned "true tendon thickness" concept [13, 14] (**Fig. 2**). Paratendinous neovascularizations with diffuse ingrowing of capillaries and arterioles are often seen histopathologically in the case of degenerated tendons [1]. In the case of achillodynia (pain syndrome of the Achilles tendon), Doppler sonography typically shows intratendinous neovascularizations but these can also be visualized in asymptomatic tendons [15] (**Fig. 2**). The percentage of asymptomatic tendons with intratendinous neovascularizations is up to 35 % according to the literature [25]. The degree of neovascularization can be classified according to the Öhberg score (0 through 4 +) with 0 indicating the absence of neovascularization, 1 + the presence of neovascularization in the anterior tendon segment and 2 + through 4 + indicating varying degrees of irregular neovascularization [26]. The modified Öhberg score is as follows: 0 (no vessels), 1 + (1 vessel in the anterior segment, 2 + (2 vessels in the entire tendon), 3 + (3 vessels), and 4 + (> 3 vessels) [27]. The existence of a correlation between the occurrence of pain and the degree of neovascularizations is a topic of debate in the literature due to the relatively high prevalence of neovascularizations in asymptomatic tendons [15, 28].

Since mucoid and hypoxic degeneration can coexist, a qualitative differentiation is often difficult [29].

Lipomatous degeneration can be diffuse or focal. Diffuse structure changes or hypoechogenic zones are often seen in ultrasound as a sign of local xanthomas [30]. MRI shows point-shaped hyperintensities in the T2 and T1 weighting. The tendon can also appear thickened in the case of lipomatous atrophy. Differentiation from other types of tendinopathy can be difficult [31]. Calcifying tendinosis often includes focal calcifications of the tendon which appear extremely hyperechogenic with a lack of dorsal through-transmission in sonography. In MRI, calcifications may exhibit a signal behavior corresponding to the bone marrow of the tibia in the T1 weighting [6].

Partial rupture

On the whole, the diagnosis of partial ruptures via ultrasound is limited with the differentiation from focal degenerative changes being particularly difficult [32].

Ultrasound shows partial ruptures of the Achilles tendon as wavy irregularities of the fibrillar echo pattern [33]. Focal hypoechogenic areas and thickening of the affected tendon segment are often seen [32]. Alfredson et al. reported that the superficial dorsal tendon boundary also has an interruption and accompanying hyperperfusion can be visualized with power Doppler [33]. However, sonographic diagnosis of a partial rupture seems to be limited in particular in the myotendinous junction and in the proximal third of the Achilles tendon. Supplementary MRI is usually necessary in this case [34].

In the case of a partial rupture, MRI shows apposition of the ruptured fibers and local signal enhancement in particular in T1 and T2-weighted imaging [23]. Moreover, partial ruptures exhibit significant focal thickening of the Achilles tendon to 10 – 18 mm, which is often greater than the thickening associated with degenerative tendinosis [35]. However, the differentiation between a small partial rupture and focal degenerative changes remains a challenge both with sonography and MRI [36] (**Fig. 2**).

Complete rupture

In the case of a complete rupture, a differentiation can be made between an acute complete rupture and a chronic rupture with scar formation [24]. Acute as well as chronic rupturing of the Achilles tendons often shows concurrent degenerative changes [35]. Ruptures usually occur in the

avascular area 2 – 6 cm proximal to the calcaneal tendon insertion. Moreover, atypical insertional or proximal Achilles tendon ruptures can occur in rare cases. Changes near the insertion often occur as part of an advanced insertional tendinopathy, while proximal ruptures usually correspond to a rupture of the muscle-tendon complex [6] (**Fig. 3**).

Complete rupture of the Achilles tendon is visualized sonographically as dehiscence of the fibers with a frequently inhomogeneous hypoechoic hematoma between the tendon stumps [32, 37]. In the chronic stage, fiber discontinuity occurs with structure resolution which exhibits variable echogenicity depending on the chronicity of the process [38]. A hyperechogenic signal indicates scar formation (fibrosis) [39]. The interruption of the tendon structure and variable dislocation of the tendon stumps can be effectively visualized with MRI [24]. A concomitant hematoma with edema formation and very high signal intensity in T2 weighting is often seen [6, 23]. Chronic ruptures are typically low signal in T1 weighting, and discontinuity of the tendon with horizontal hyperintensity is often seen in T2 weighting [24, 38].

Insertional tendinopathy

Insertional tendinopathy which accounts for only approx. 20 % of all tendinopathies of the Achilles tendon is rarer than tendinosis [1].

Insertional tendinopathy is visualized in ultrasound as tendinous thickening in the region of the tendon insertion. Hook-shaped calcifications with a lack of dorsal through-transmission or pathological bone spur formation (dorsal calcaneal spur) can often be delineated. T2-weighted MRI shows fine longitudinal hyperintense lines corresponding to focal microtears [24] (**Fig. 4**). Moreover, concomitant changes, such as bone marrow edema of the calcaneus (8 %) or a thickened retrocalcaneal bursa (19 %), can be imaged [40, 41]. MRI has proven to be very useful for insertional tendinopathy treatment planning and monitoring in a number of studies [42, 43].

Peritendinous changes

Paratenonitis

Paratenonitis and peritendinitis are often used synonymously and refer to the inflammatory change of the paratenon which surrounds the Achilles tendon and separates it from the crural fascia [1]. The paratenon differs from the peritendineum of other tendons in that it is not a real tendon sheath. It does not contain any synovial tissue but does supply blood to the tendon, which is the basis for inflammatory changes [6]. Therefore, the term paratenonitis better describes the inflammatory reaction of the tissue around the actual tendon.

Due to the increased fluid content in the inflamed tissue, T2-weighted MRI shows paratenonitis as a bright hyperintense band that typically incompletely surrounds the Achilles tendon [22, 24]. In contrast, ultrasound shows paratenonitis as a dark hypoechogenic peritendinous halo due to the reduced echogenicity. Once the condition has become chronic, irregularities of the boundary zone of the paratenon can additionally occur and result in significantly increasing hypervascularization in power Doppler [44, 45] (**Fig. 2**).

Retrocalcaneal bursitis

The retrocalcaneal bursa is located between the calcaneal tuberosity and the Achilles tendon insertion and is surrounded by Kager's fat pad. It is directly related to the paratenon and is often also affected in the case of degenerative tendon changes [46]. In these cases, the bursa often exhibits histological degeneration of the bursal wall – at times with calcification or hypertrophy – and intraluminal fluid collection. In sonography, the fluid-filled bursa appears homogeneously hypoechogenic, while it appears hyperintense in T2-weighted MRI [45]. However, focal hyperintensity of the bursa is not to be primarily evaluated as pathological. The bursa in asymptomatic subjects reaches an average size of 1 × 6 × 3 mm while the symptomatic bursa is usually significantly larger at approx. 4 × 9 × 4 mm [46]. In addition to the retrocalcaneal bursa, the subcutaneous calcaneal bursa, which is directly subcutaneous and posterolateral to the bony insertion, is frequently also affected. In a pathological state, it appears as an elongated hypoechogenic structure in sonography and as a hyperintense structure in T2-weighted MRI [45] (**Fig. 4**).

Haglund's exostosis

Haglund's deformity is caused by a pathological impingement of the retrocalcaneal bursa and the insertional Achilles tendon. The most important influencing factors in this context are an inherent prominence of the posterolateral portion of the calcaneus and the wearing of high-heeled shoes ("pump bump"). In the case of repetitive injuries to the insertion region, hypertrophy of the calcaneal tuberosity, frequently with concomitant bursitis and tendinopathy, occurs. Signs of bursitis and insertional tendinosis and a prominent, cranially extended posterior tuberosity are typically visualized [6, 22, 47] (**Fig. 4**).

Clinical radiological tendinopathy classifications

For radiological imaging in the clinical routine, different clinical presentations of acute or chronic overuse injuries of the Achilles tendon must be considered. Schweitzer und Karasick differentiate between 7 clinically relevant main groups including a total of 11 subgroups with different imaging characteristics [22]. The individual groups differ with respect to their location (insertion, peritendinous and intratendinous changes), morphology (rupture, calcification, hypoxic and mucoid degeneration), and chronicity (acute versus chronic). In a recently published study, Weber et al. reduced these to 4 clinically relevant groups based on morphological imaging criteria (1) peritendinous changes (paratenonitis), (2) increase in the size of the Achilles tendon (hypoxic degeneration) with focal intratendinous changes, (3) visible morphological changes in the case of mucoid degeneration (e. g. signal amplification in T2 weighting), and (4) ruptures. Moreover, the differentiation between insertional and non-insertional tendinopathies (mid-portion tendinosis) seems to be important [1, 22, 24]. Viewed with other clinical and morphological imaging criteria, the following points therefore seem relevant:

- Location: Peritendinous, intratendinous insertional, or intratendinous non-insertional

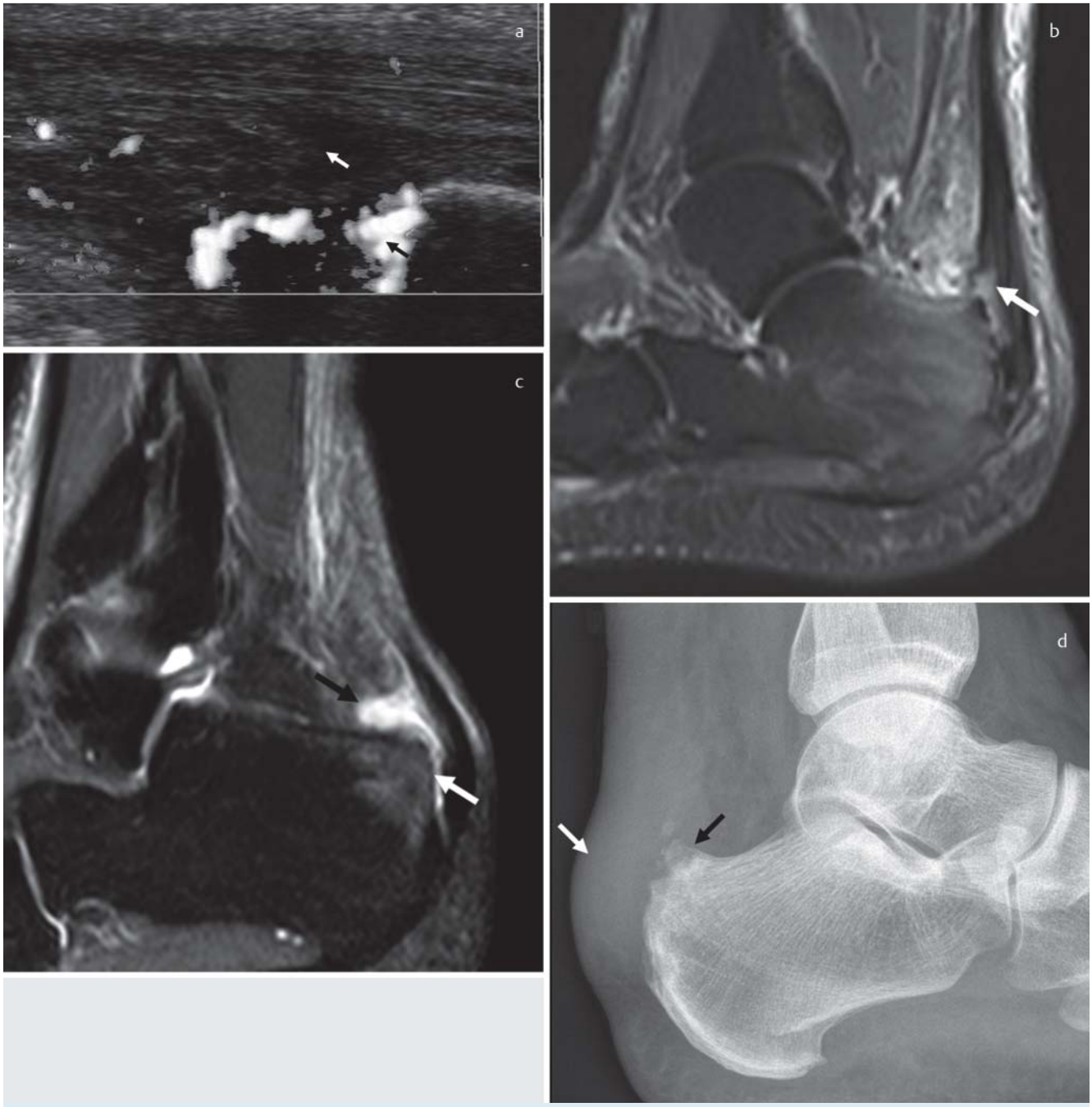

Fig. 4 **a** shows an insertional tendinopathy with retrocalcaneal bursitis in a 55-year-old patient. The Achilles tendon shows an insertional thickening with focal hypoechoic areas (white arrow). The black arrow marks the concomitant hyperemia of the retrocalcaneal bursa. **b** shows a PD weighted sagittal image of an insertional tendinopathy in a 75 years old patient, where focal hyperintensities are present (white arrow). **c** Sagittal PD-weighted image with fat saturation in a 26-year-old patient with acute retrocalcaneal bursitis (black arrow). The bursa is enlarged (18 × 9 mm) and shows a hyperintense signal (fluid) in the PD-weighted image. Accompanying bone bruise within the proximal part of the calcaneal tuberosity is also present (white arrow). A plain radiograph **d** of a symptomatic Haglund's deformity (black arrow) in a 50-year-old female patient with accompanying swelling of the adjacent subcutaneous tissue (white arrow).

- Morphology: Increase in caliber (hypoxic degeneration) vs. generalized structural changes (mucoid degeneration)
- Chronicity: Acute versus chronic tendinopathy

In comparison to the above-described classification according to Schweitzer and Karasick, other classification systems (e.g. according to Weinstabl et al. or Pomeranz et al.) are based on the extent of the visible morphological changes [43, 48, 49]. To summarize, we find the following classification useful for the clinical routine:

1. Solitary paratenonitis: Strict peritendinous changes without intratendinous involvement.
2. Tendinosis without or with only mild visible morphological intratendinous structural changes: Thickening of the tendon with only focal signal alterations of the ten-

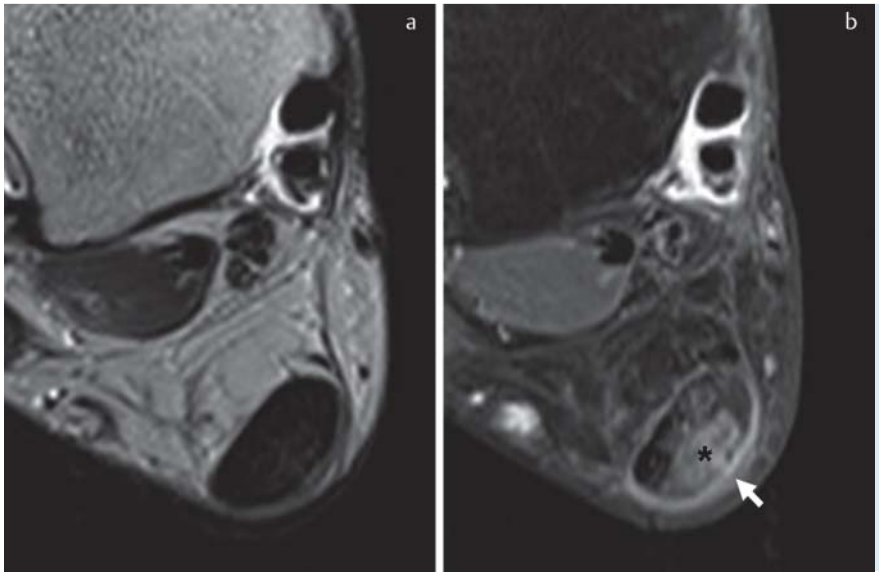

Fig. 5 **a** PD-weighted axial image of a 46-year-old patient with mid-portion tendinosis.In comparison, **b** shows a contrast-enhanced axial T1-weighted image with fat saturation. Distinct intratendinous and paratendinous contrast enhancement (black asterisk and white arrow) is present.

don corresponding to hypoxic degeneration, possibly with concomitant paratenonitis.

3. Tendinosis with visible morphological intratendinous structural changes: Resolution of the fibrillar echo pattern, signal enhancement in T2 weighting corresponding to mucoid degeneration ("silent tendonitis") according to Karasek et al.
4. Ruptures: Complete and partial rupture.
5. Insertional tendinopathy: This is often considered an independent entity and is often accompanied by focal calcifications [1].

In contrast to chronic changes, paratenonitis, bone marrow edema at the calcaneal insertion, edema of Kager's fat pad, and concomitant retrocalcaneal bursitis are often present in the case of an acute tendinopathy [22, 24]. The use of power Doppler ultrasonography which shows increased vascularization of the peritendinous structures in the case of an acute tendinopathy seems useful in this regard.

Despite the above criteria and classifications of Achilles tendon changes, definitive diagnosis of pathologies on a purely morphological basis remains difficult. This is due to the fact that types of hypoxic and mucoid degeneration can be histologically present in both asymptomatic and symptomatic tendons and the line between borderline normal changes and borderline pathological changes is not clearly defined [29]. Therefore, Weber et al. recently used MRI images to evaluate various quantitative parameters in addition to visible morphological characteristics to increase the sensitivity and specificity for the diagnosis of pathologies in the region of the Achilles tendon. Using 3 parameters (anteroposterior diameter of Achilles tendon 3 cm above the calcaneus, craniocaudal size of the retrocalcaneal bursa, elliptical tendon cross-section from maximum anteroposterior and mediolateral diameter), it was possible to differentiate between healthy (i. e., asymptomatic) and pathological (i. e., symptomatic) changes in the Achilles tendon with a specificity of 91 % and a sensitivity of 97 % [24]. However, the degree of intratendinous and peritendinous changes was not applied to the binary logistic regression analysis. Other studies using comparable parameters for differentiating between symptomatic and asymptomatic tendons (tendon volume in MRI [50, 51] and average tendon thickness 2 – 3 cm from the calcaneus in the longitudinal ultrasound image [14]) yielded similar results. However, the relevance of the parameters in the evaluation of clinical course, especially the persistence of visible morphological changes after acute symptoms have subsided, remains unclear [52]. Quantitative parameters for characterizing the intratendinous structure could respond earlier to changes than only the determination of tendon diameter or cross-sectional area and therefore prove to be more sensitive for follow-up during treatment or for the diagnosis of the early stages of degeneration. With respect to these remaining diagnostic shortcomings, a number of parameters have been evaluated in recent years with varying degrees of success. The most important methods in current research regarding this topic are described briefly in the following and evaluated with respect to their clinical relevance.

New possibilities for imaging the Achilles tendon

Contrast-enhanced MRI

In addition to the routine use of native T1, T2, or PD-weighted sequences in MRI, intravenously administered contrast agents can also be used in special cases. However, the results of different studies regarding this topic are controversial. While Movin et al. postulated an improved detection of symptomatic tendons compared to asymptomatic tendons, Gardin et al. did not find a benefit with respect to native imaging [36, 53]. They achieved the best differentiation regarding the intratendinous signal behavior in a native T1-weighted gradient echo sequence. Both studies are comparable only on a limited basis with respect to the study protocol and are only of limited significance due to the small number of patients (20 and 25 patients, respectively). The asymptomatic tendons of the patients served as the control in each case [36, 53]. Shalabi et al. examined the contrast agent dynamics in 15 patients with symptomatic tendinopathy of the Achilles tendon. The healthy tendons on the opposite side served as the control group (n = 10). The symptomatic tendons exhibited early contrast uptake with-

out washout in the late phases while the control group only showed uptake in the late phase [54]. A disadvantage of intravenous contrast-enhanced MRI is the potential risk for nephrogenic systemic fibrosis (NSF) in the case of significantly limited kidney function and the potential allergenic effect, thus making large studies with healthy subjects problematic. According to the current data, there is no clear clinically relevant benefit of the use of intravenous contrast agent. Therefore, routine application should be viewed with reservation. Intravenous application of contrast agent should only be used for evaluating the Achilles tendon when indicated by a concomitant disease (e. g. rheumatoid arthritis, Bechterew's disease).

Automated contour recognition and texture analysis

An important clinical parameter in the diagnosis of tendinosis, i. e., the maximum thickness of the Achilles tendon, is typically determined via a manual point-wise measurement both in ultrasound and MRI images [13, 55]. However, in particular in regard to the measurement of small tendon changes, point-wise manual measurement is only usable on a conditional basis due to its limited reproducibility (variation coefficient approx. 5 – 7 %) [13, 14, 55]. Automated contour recognition methods improve reproducibility by up to 50 % in both B-mode ultrasound and MRI [14, 50, 51]. Moreover, the maximum thickness as well as the tendon volume can be reliably calculated in an automated manner via so-called seed growing or snake algorithms in MRI images (variation coefficient approx. 1 – 5 %) [50, 51]. The automated methods could have particular advantages with respect to the detection of the smallest tendon changes, e. g. with respect to minor training or therapy effects. A disadvantage is that some methods are still dependent on image quality and require manual corrections by an experienced examiner in individual cases [14, 50, 51]. In addition to surface area and volume calculation, the automated methods also allow more comprehensive computed-aided analysis of the internal tendon structure. A possible parameter with good reproducibility is the average signal intensity of the Achilles tendon in MRI images [50]. Another study showed a good correlation between intratendinous signal enhancement and the pain symptoms experienced by the patients with the pain symptoms correlating better with the signal intensity than the tendon volume [53].

Bashford et al. developed an ultrasound-based method for automated differentiation of degenerative and healthy Achilles tendons. Quadratic regions of interest (ROIs) were split into their spatial frequency spectrums and 8 different spatial frequency parameters were extracted. Up to 84.9 % of patients with a tendinopathy were able to be correctly classified in discriminant analysis [56]. In contrast, Van Schie et al. used an automated ultrasound tissue characterization (UTC) to examine four different, predefined echo patterns based on stability and distribution (1: very stable, 2: average stability, 3: highly variable, 4: low intensity with variable distribution). It was shown that symptomatic Achilles tendons with tendinosis have a significantly higher percentage of variable unstable echo patterns compared to a healthy control collective [57].

Because of the low number of examined patients, automated texture analysis must still be considered in terms of experimental feasibility studies and has not become established in routine imaging due to the questionable therapeutic consequence. This does not apply to automated contour recognition which is based on already clinically established measurement methods (Achilles tendon thickness and volume) and significantly reduces the examiner-dependent variability so that it could become a valuable part of the clinical routine particularly for follow-up examinations.

Elasticity analysis

Real-time sonoelastography of the Achilles tendon has been a topic of research for a number of years [58, 59]. The different degrees of tissue hardness and elasticity are visualized using a color scale in the corresponding B-mode image [58]. De Zordo et al. showed that, in contrast to healthy tendons which have a very hard structure (93 % hard), tendon degeneration is accompanied by increasing softening of the structure (57 % soft) [60]. In opposition to the study by Zordo, Sconfienza et al. were able to show that symptomatic Achilles tendons of athletes have a higher degree of tendon structure hardness but the data were also only evaluated qualitatively in this study [61]. Drakonaki et al. attempted to quantify the tendon structure elasticity and introduced the so-called strain index which is the ratio between the tendon tissue hardness and the hardness of the surrounding fat tissue [59]. However, with a variation coefficient of approx. 30 % for different examiners, the reproducibility is too low for clinical diagnostics.

Velocity-encoded phase-contrast MRI (VE-PC-MRI) in combination with an MR-compatible interferometer is another option for the in vivo quantification of force-dependent length changes and stiffness properties of the Achilles tendon. In this way Shin et al. were able to determine the force-length curve of the Achilles tendon in the case of isometric contractions [62]. For the reproducibility of the transition point (change of the tendon length in mm at 40 N), there was good reproducibility with a variation coefficient of approx. 4 % (intraday variability). However, the variation coefficient was significantly higher at approx. 17 % (intraday variability) for the stiffness measurement [62]. Since there is currently no data regarding pathologically altered tendons with respect to VE-PC-MRI, a final conclusion about clinical applicability cannot be made.

Due to the very small number of test subjects in the studies regarding measurement with both sonoelasticity and VE-PC-MRI, the applicability of the data is still limited. Clinically relevant use is not in sight at this time.

"Magic angle" and ultrashort echo time (UTE) imaging

In conventional MR sequences, the healthy Achilles tendon appears largely homogeneously signal-free. This is due to the extremely short T2 relaxation time of approx. 1 ms which causes almost complete dephasing of the transverse magnetization prior to the actual data acquisition [63]. The short T2 times are primarily based on the dipole-dipole interactions between the highly organized collagen fibers and the interstitial water molecules embedded between them. The strength of the dipole-dipole interaction depends on the orientation (angle θ) with respect to the B0 field and is defined by the formula $(3^{*}\cos^{2}\theta - 1)$. At an angle of 54.74°, the so-called magic angle, the strength of the dipole-dipole interaction is minimal, resulting in an exten-

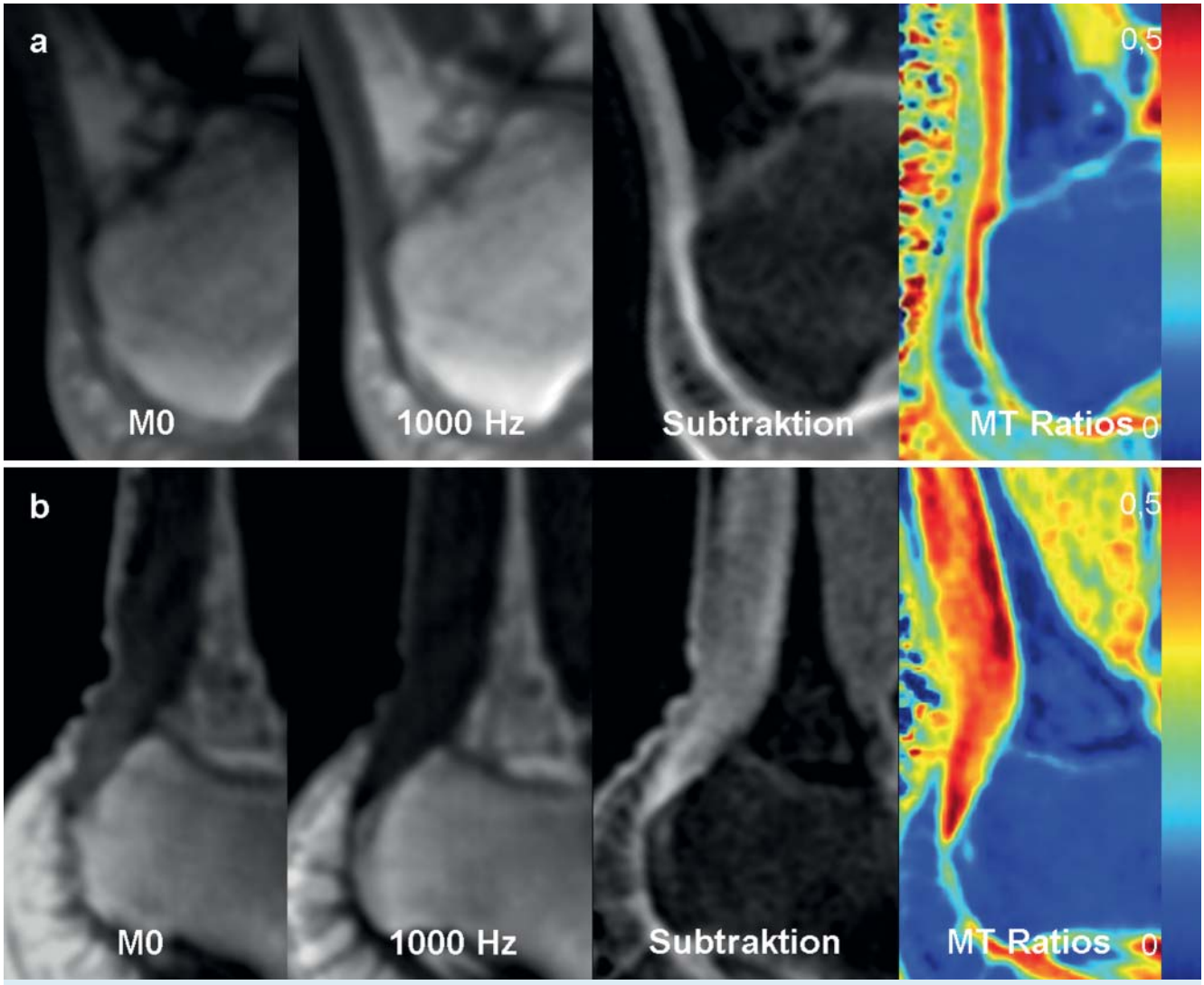

Fig. 6 shows sagittal 3 D UTE images with (off-resonance frequency 1 kHz) and without off-resonance saturation pulse (M0) and the respective subtraction image. Pixel-wise calculated MTR parameter maps are also shown. **a** shows the images of a healthy Achilles tendon of a 31-year-old volunteer. In contrast, **b** shows images of a 44-year-old patient with mid-portion tendinosis and focally decreased MTR values.

sion of the T2 relaxation by a factor of approximately 100. As a result, the tendon tissue with a fiber orientation of approx. 55° with respect to the B0 field is visualized as signal intense [63, 64]. In a number of clinical studies, it was shown that degenerative and acute changes of the Achilles tendon can be better delineated with non-contrast-enhanced MR imaging with the help of the "magic angle" effect [65, 66]. Moreover, Oatridge et al. and Marshall et al. showed that a pathological contrast agent uptake in symptomatic tendons that was not able to be visualized with parallel orientation to the B0 field can be visualized with the help of the "magic angle" effect [66, 67]. However, in the case of minimal random samples, the applicability of the above studies is limited. The utilization of the "magic angle" effect is a simple means of intratendinous signal enhancement but the positioning of the patient's lower leg at an angle of approx. 55° with respect to the B0 field when using a conventional tube-shaped MR scanner and conventional extremity coils is a challenge.

In addition to "magic angle" imaging, the introduction of so-called ultrashort echo time (UTE) sequences also made it possible to visualize quickly relaxing tissues such as ligaments, tendons, or cortical bones, with positive contrast. In contrast to conventional MR sequences with echo times of approx. TE > 1 ms, echo times of approx. TE = 0.05 ms can be achieved with UTE sequences. To achieve such a reduction of the minimum echo time, different methods, such as shortening of the HF pulse time or the use of unconventional read-out samplings, are combined [68]. On the one hand, UTE imaging with its ultrashort echo times provides an amplified intratendinous signal and improved visualization of pathologies both in the native imaging method and in contrast-enhanced sequences [69]. On the other hand, UTE sequences also allow quantitative evaluation of different MR-specific tissue characteristics. Essentially, known methods have been applied to UTE imaging so that in particular T1, T1rho, T2* and magnetization transfer (MT) effects can be evaluated [70–75].

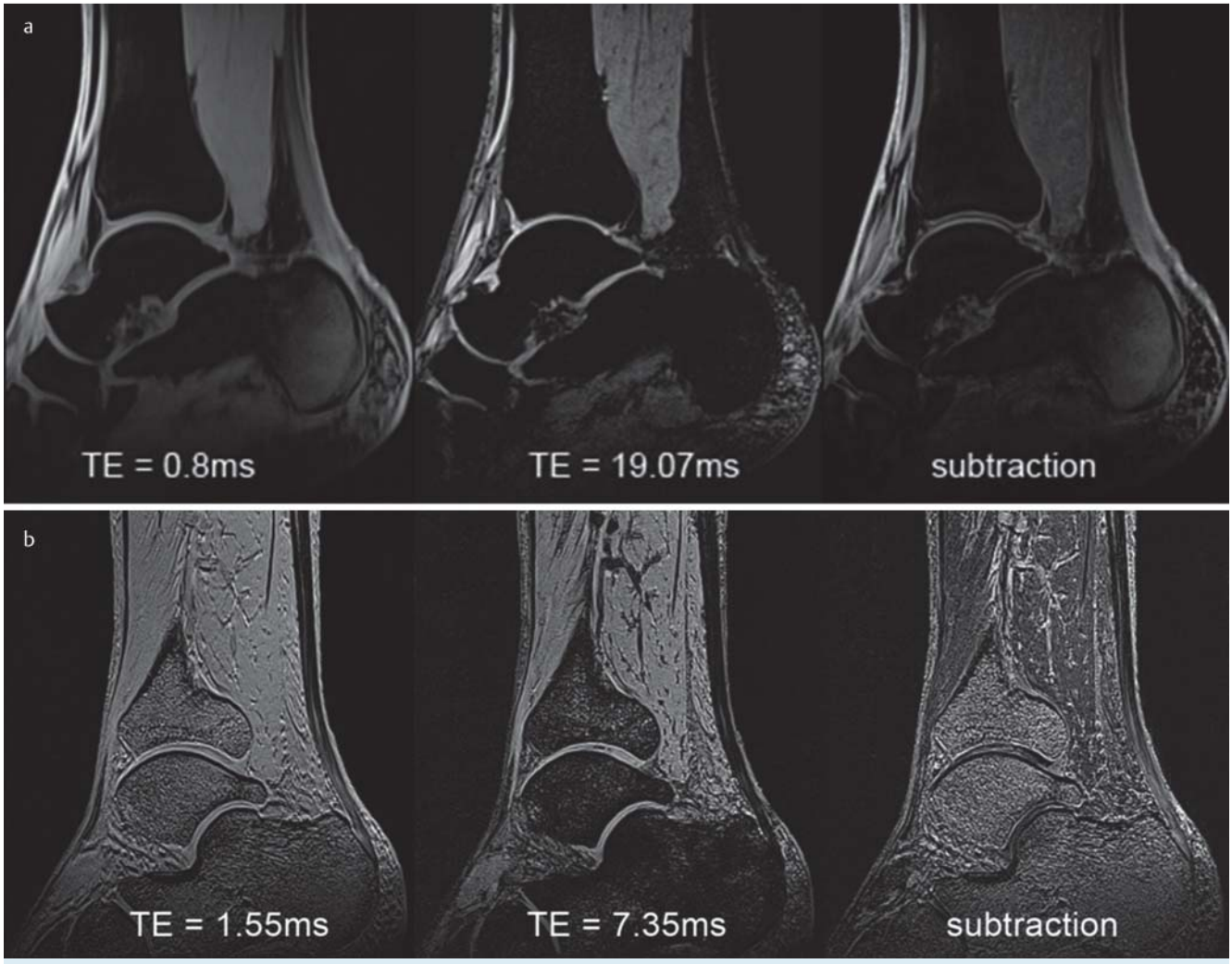

Fig. 7 shows sagittal MR images of an Achilles insertional tendinopathy in a 39-year-old patient at 3 T **a** and 7 T **b**. Images with different echo times and a corresponding subtraction image are presented (courtesy of Prof. Trattnig and co-workers, Vienna, Austria).

In a number of studies, the effective transverse relaxation time (T2*) of healthy and degenerative tendons was examined. Differences in the T2* relaxation time were seen both in healthy and degenerated tendons depending on the tendon region (e. g. insertion, muscle-tendon complex, mid-portion) [73, 74]. In studies assuming a monoexponential signal decay, the T2* time at 3 T in the mid-portion of a healthy Achilles tendon in vivo was approx. 1.5 ms [74, 76]. However, more recent studies regarding the T2* effect assume a biexponential signal decay from which a long and short T2* component can be derived [70, 73]. In healthy tendons, the fractional portion of the short T2* component at 3 T (0.5 – 1.3 ms depending on the region and study) is approximately 50 – 80 % and that of the long T2* component (7.9 – 31.8 ms) is 20 – 50 % [70, 73]. The longitudinal relaxation time of the Achilles tendon was also determined in vivo via UTE sequences and is approx. 700 ms [75]. So-called T1rho effects were evaluated as a further parameter by Du et al. using spinlock pulses [71, 77]. However, further studies regarding T1, T2*, and T1rho effects at 3 T for degenerative Achilles tendons in vivo are currently not available. Therefore, their clinical significance is uncertain.

Another well known effect is based on the so-called magnetization transfer (MT) which occurs in tissues with a high percentage of macromolecules. This can be determined in tissues with very short transverse relaxation times with the help of UTE sequences. Using select and varied parameters, both the amount of free and bound water and the exchange constants can be quantified and used as absolute parameters. A simpler possibility that is much more suitable for the clinical routine is the pixel-wise calculation of a so-called MT quotient from the images with and without an MT preparation pulse [72, 74]. Tendons with symptomatic tendinosis have significantly lower MT quotients than healthy or asymptomatic tendons [72] (**Fig. 6**). Moreover, it is interesting that tendons with asymptomatic tendinosis and pure paratenonitis also have slightly reduced MT ratios indicating a concomitant tendon injury [72].

Possibilities of imaging at 7 T

In the case of the MR sequences used in the clinical routine, significantly better SNR and contrast-to-noise ratio (CNR) were achieved at 7 T compared to 3 T due to the improved resolution in the ultrahigh field at 7 T [78] (**Fig. 7**). Juras

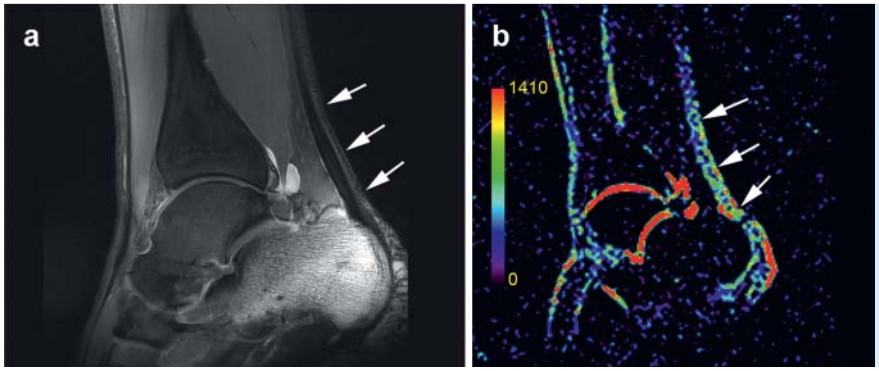

Fig. 8 shows a conventional sagittal 1H MR image **a** in comparison to 23Na imaging **b** in a 39-year-old patient with insertional tendinopathy at 7 T. A diffuse sodium distribution is present within the Achilles tendon, which is marked by white arrows (courtesy of Prof. Trattnig and co-workers, Vienna, Austria).

Table 2 Overview of typical imaging features of common intra- and peritendinous pathologies associated with overuse.

diagnosis pathology	B-mode ultrasound	Power Doppler/color Doppler	MRI	CE MRI	UTE	elasticity
intratendinous changes						
tendinosis	thickening of the tendon (6 – 7 mm) focal hypoechogenicity	neovascularization (initially in the anterior portion)	thickening with increase in volume alteration with focal hyperintensities in T2w	increased contrast enhancement; significant increase in contrast agent dynamics	focal extension of short T2* components significantly reduced MT ratio (1 – 5 kHz)	controversial: increasing vs. decreasing hardness
partial rupture	thickening of the tendon (10 – 18 mm) interrupted fibrillar echo texture	concomitant focal hyperperfusion	apposition of the fibers, increased intensity in T1w, significantly increased intensity in T2w	n.a.	n.a.	n.a.
chronic rupture	scar formation with interruption of the echo texture, focal hypoechogenicity as well as hyperechogenicity	neovascularization	horizontal focal signal enhancement in T2w, No increased signal intensity in T1w	n.a.	n.a.	n.a.
acute rupture	complete discontinuity of the fibers, intratendinous hematoma (hypoechoic to inhomogeneously echoic)	concomitant focal hyperperfusion	apposition and dehiscence of the fibers over the entire tendon width, increased intensity in T1w, significantly increased intensity in T2w	n.a.	n.a.	n.a.
insertional tendinopathy	insertional thickening with irregular echo pattern, focal calcifications	neovascularization	signal alterations in T2w, insertional thickening	n.a.	n.a.	n.a.
peritendinous changes						
paratenonitis	partial ring-shaped peritendinous hypoechogenicity	increased vascularization	partial ring-shaped hyperintensity in T2w and TIRM	n.a.	moderately reduced MT ratio (1 – 5 kHz)	n.a.
retrocalcaneal bursitis	focal hypoechogenicity cranial to retrocalcaneal tuberosity	concomitant focal hyperperfusion	significant focal hyperintensity in T2w and TIRM	n.a.	n.a.	n.a.

MRI = magnetic resonance imaging; CE = contrast-enhanced; UTE = ultrashort echo time; T2w = T2 weighting; TIRM = turbo inversion magnitude; n.a. = not available; MT = magnetization transfer.

et al. used a 3 D UTE sequence to examine the biexponential T2* signal decay in different portions of the Achilles tendon (insertion, mid-portion, muscle-tendon complex) in healthy and degenerated tendons at 3 T and 7 T. Significant differences in the T2* signal decay were seen depending on the examined region or with respect to healthy and degenerated tendons [73]. In addition to the ^{1}H-MRI used in the clinical routine, other atomic nuclei such as ^{23}Na can be used with restrictions for imaging in scientific studies. There was a good correlation to the water and proteoglycan content of the examined ex vivo preparations for the SNR in the histological comparison [79]. Moreover, initial in vivo

results show a good correlation with the proteoglycan content of healthy and degenerated Achilles tendons and should be further evaluated in larger clinical studies [80] (**Fig. 8**). Due to the highly limited clinical availability of MRI units with a basic field strength of 7 T and the not yet fully developed ultrahigh field examination technology, use in the clinical routine is currently not foreseeable [78].

Conclusion

For the clinical routine, an evaluation of the exact location of visible morphological changes seems to be relevant for the differentiation between peritendinous changes (paratenonitis) and intratendinous changes (tendinosis and insertional tendinopathy) (**Table 2**). For further evaluation, sonography as well as MRI can be used to differentiate between different types of degeneration, mainly hypoxic degeneration (with thickening of the tendon and minor focal structure changes) and mucoid degeneration (with changed echo texture and pathological MR signal behavior) but the line between the two is not clearly defined. Concomitant peritendinous changes such as paratenonitis or retrocalcaneal bursitis as well as bone marrow edema of the calcaneus make it possible to make a qualitative statement about acuteness. These peritendinous changes can also be reliably diagnosed via MRI or via ultrasound plus power Doppler except for in the case of bone marrow edema. Acute and chronic complete ruptures can also be effectively and reliably diagnosed with both methods. However, the diagnosis of partial ruptures which can sometimes be missed in morphological imaging diagnostics depending on location (proximal in particular in this case) and degree is currently still problematic. MRI seems to be superior to ultrasound in this regard.

In addition to qualitative morphological imaging criteria, supplementary quantitative criteria (Achilles tendon thickness 2 – 3 cm above the calcaneus) or the planimetry/volumetry of the Achilles tendon seem to be significant with respect to the differentiation between symptomatic and asymptomatic Achilles tendons. In addition, automation of the corresponding measurement methods allows simple and reliable examiner-independent evaluation also for follow-up. However, it is still unclear whether these measurement variables are suitable for the evaluation of therapy effectiveness or the diagnosis of the onset of degenerative changes. This diagnostic gap could be filled by newer, quantitatively determinable parameters of the intratendinous structure. However, larger clinical studies with corresponding follow-up are needed to be able to come to a clear conclusion about clinical relevance in this case.

Acknowledgment

We thank Professor Trattnig and Mr. Juras for the MR images of the Achilles tendon of 7 Tesla.

References

1 *Paavola M, Kannus P, Jarvinen TA et al.* Achilles tendinopathy. J Bone Joint Surg Am 2002; 84: 2062 – 2076
2 *Riley G.* The pathogenesis of tendinopathy. A molecular perspective. Rheumatology 2004; 43: 131 – 142
3 *Cheung Y, Rosenberg ZS, Magee T et al.* Normal anatomy and pathologic conditions of ankle tendons: current imaging techniques. Radiographics 1992; 12: 429 – 444
4 *Kälebo P, Goksör L, Swärd L et al.* Soft-tissue radiography, computed tomography, and ultrasonography of partial Achilles tendon ruptures. Acta Radiol 1990; 31: 565 – 570
5 *Ohashi K, El-Khoury GY, Bennett DL.* MDCT of Tendon Abnormalities Using Volume-Rendered Images. American Journal of Roentgenology 2004; 182: 161 – 165
6 *Pierre-Jerome C, Moncayo V, Terk MR.* MRI of the achilles tendon: A comprehensive review of the anatomy, biomechanics, and imaging of overuse tendinopathies. Acta Radiologica 2010; 51: 438 – 454
7 *Pavlov H, Heneghan MA, Hersh A et al.* The Haglund syndrome: initial and differential diagnosis. Radiology 1982; 144: 83 – 88
8 *Martinoli C, Bianchi S, Dahmane M et al.* Ultrasound of tendons and nerves. Eur Radiol 2002; 12: 44 – 55
9 *O'Connor PJ, Grainger AJ, Morgan SR et al.* Ultrasound assessment of tendons in asymptomatic volunteers: a study of reproducibility. Eur Radiol 2004; 14: 1968 – 1973
10 *Grassi W, Filippucci E, Farina A et al.* Sonographic imaging of tendons. Arthritis Rheum 2000; 43: 969 – 976
11 *Kainberger F, Frühwald F, Engel A et al.* Die Sonographie der Achillessehne und ihres Gleitlagers. Fortschr Röntgenstr 1988; 148: 394 – 397
12 *Fornage BD.* The hypoechoic normal tendon. A pitfall. Journal of Ultrasound in Medicine 1987; 6: 19 – 22
13 *Fredberg U, Bolvig L, Andersen NT et al.* Ultrasonography in evaluation of Achilles and patella tendon thickness. Ultraschall in Med 2008; 29: 60 – 65
14 *Syha R, Peters M, Birnesser H et al.* Computer-based quantification of the mean Achilles tendon thickness in ultrasound images: effect of tendinosis. Br J Sports Med 2007; 41: 897 – 902
15 *Sengkerij PM, de Vos RJ, Weir A et al.* Interobserver reliability of neovascularization score using power Doppler ultrasonography in midportion achilles tendinopathy. Am J Sports Med 2009; 37: 1627 – 1631
16 *Richards PJ, Win T, Jones PW.* The distribution of microvascular response in Achilles tendonopathy assessed by colour and power Doppler. Skeletal Radiology 2005; 34: 336 – 342
17 *Collins MS, Felmlee JP.* 3T magnetic resonance imaging of ankle and hindfoot tendon pathology. Top Magn Reson Imaging 2009; 20: 175 – 188
18 *Gold GE, Han E, Stainsby J et al.* Musculoskeletal MRI at 3.0 T: relaxation times and image contrast. Am J Roentgenol 2004; 183: 343 – 351
19 *Mantel D, Flautre B, Bastian D et al.* Structural MRI study of the Achilles tendon. Correlation with microanatomy and histology. J Radiol 1996; 77: 261 – 265
20 *Aström M, Rausing A.* Chronic Achilles tendinopathy. A survey of surgical and histopathologic findings. Clin Orthop Relat Res 1995; 316: 151 – 164
21 *Leadbetter WB.* Cell-matrix response in tendon injury. Clin Sports Med 1992; 11: 533 – 578
22 *Schweitzer ME, Karasick D.* MR Imaging of Disorders of the Achilles Tendon. American Journal of Roentgenology 2000; 175: 613 – 625
23 *Stiskal M, Neuhold A, Weinstabl R et al.* MR-tomographische Befunde bei Achillodynie. Fortschr Röntgenstr 1990; 153: 9 – 13
24 *Weber C, Wedegärtner U, Maas LC et al.* MR-Tomografie der Achillessehne: Evaluation von Kriterien zur Differenzierung von asymptomatischen und symptomatischen Sehnen. Fortschr Röntgenstr 2011; 183: 631 – 640
25 *Hirschmüller A, Frey V, Deibert P et al.* Powerdopplersonografische Befunde der Achillessehnen von 953 Langstreckenläufern – eine Querschnittsstudie. Ultraschall in Med 2010; 31: 387 – 393
26 *Öhberg L, Alfredson H.* Ultrasound guided sclerosis of neovessels in painful chronic Achilles tendinosis: pilot study of a new treatment. British Journal of Sports Medicine 2002; 36: 173 – 175
27 *de Vos RJ, Weir A, Cobben LPJ et al.* The Value of Power Doppler Ultrasonography in Achilles Tendinopathy. The American Journal of Sports Medicine 2007; 35: 1696 – 1701
28 *Zanetti M, Metzdorf A, Kundert HP et al.* Achilles Tendons: Clinical Relevance of Neovascularization Diagnosed with Power Doppler US1. Radiology 2003; 227: 556 – 560

29 *Haims AH, Schweitzer ME, Patel RS et al.* MR imaging of the Achilles tendon: overlap of findings in symptomatic and asymptomatic individuals. Skeletal Radiology 2000; 29: 640 – 645
30 *Tsouli SG, Xydis V, Argyropoulou MI et al.* Regression of Achilles tendon thickness after statin treatment in patients with familial hypercholesterolemia: an ultrasonographic study. Atherosclerosis 2009; 205: 151 – 155
31 *Dussault RG, Kaplan PA, Roederer G.* MR imaging of Achilles tendon in patients with familial hyperlipidemia: comparison with plain films, physical examination, and patients with traumatic tendon lesions. American Journal of Roentgenology 1995; 164: 403 – 407
32 *Paavola M, Paakkala T, Kannus P et al.* Ultrasonography in the differential diagnosis of Achilles tendon injuries and related disorders. A comparison between pre-operative ultrasonography and surgical findings. Acta Radiol 1998; 39: 612 – 619
33 *Alfredson H, Masci L, Öhberg L.* Partial mid-portion Achilles tendon ruptures: new sonographic findings helpful for diagnosis. British Journal of Sports Medicine 2011; 45: 429 – 432
34 *Kayser R, Mahlfeld K, Heyde CE.* Partial rupture of the proximal Achilles tendon: a differential diagnostic problem in ultrasound imaging. British Journal of Sports Medicine 2005; 39: 838 – 842
35 *Astrom M, Gentz CF, Nilsson P et al.* Imaging in chronic achilles tendinopathy: a comparison of ultrasonography, magnetic resonance imaging and surgical findings in 27 histologically verified cases. Skeletal Radiol 1996; 25: 615 – 620
36 *Movin T, Kristoffersen-Wiberg M et al.* MR imaging in chronic achilles tendon disorder. Acta Radiologica 1998; 39: 126 – 132
37 *Ulreich N, Huber W, Nehrer S et al.* High resolution magnetic resonance tomography and ultrasound imaging of the Achilles tendon. Wien Med Wochenschr Suppl 2002; 113: 39 – 40
38 *Maffulli N, Ajis A.* Management of Chronic Ruptures of the Achilles Tendon. The Journal of Bone & Joint Surgery 2008; 90: 1348 – 1360
39 *Harcke H, Grissom L, Finkelstein M.* Evaluation of the musculoskeletal system with sonography. American Journal of Roentgenology 1988; 150: 1253 – 1261
40 *Irwin T.* Current concepts review: insertional achilles tendinopathy. Foot Ankle Int 2010; 31: 933 – 939
41 *Karjalainen PT, Soila K, Aronen HJ et al.* MR Imaging of Overuse Injuries of the Achilles Tendon. American Journal of Roentgenology 2000; 175: 251 – 260
42 *Nicholson C, Berlet G, Lee T.* Prediction of the success of nonoperative treatment of insertional Achilles tendinosis based on MRI. Foot Ankle Int 2007; 28: 472 – 477
43 *Shalabi A.* Magnetic resonance imaging in chronic achilles tendinopathy. Acta Radiologica 2004; 45: 1 – 45
44 *Peduto AJ, Read JW.* Imaging of Ankle Tendinopathy and Tears. Topics in Magnetic Resonance Imaging 2010; 21: 25 – 36
45 *van Dijk C, van Sterkenburg M, Wiegerinck J et al.* Terminology for Achilles tendon related disorders. Knee Surg Sports Traumatol Arthrosc 2011; 19: 835 – 841
46 *Bottger BA, Schweitzer ME, El-Noueam KI et al.* MR imaging of the normal and abnormal retrocalcaneal bursae. American Journal of Roentgenology 1998; 170: 1239 – 1241
47 *Kang S, Thordarson D, Charlton T.* Insertional Achilles tendinitis and Haglund's deformity. Foot Ankle Int 2012; 33: 487 – 491
48 *Weinstabl R, Stiskal M, Neuhold A et al.* Classifying calcaneal tendon injury according to MRI findings. Journal of Bone & Joint Surgery, British Volume 1991; 73: 683 – 685
49 *Pomeranz SJ.* Foot and ankle. In: Pomeranz SJ (ed) Gamuts and pearls in MRI and orthopedics Cincinnati, OH: MRI-EFI Publ. Inc; 1997, 250 – 254
50 *Shalabi A, Movin T, Kristoffersen-Wiberg M et al.* Reliability in the assessment of tendon volume and intratendinous signal of the Achilles tendon on MRI: a methodological description. Knee Surg Sports Traumatol Arthrosc 2005; 13: 492 – 498
51 *Syha R, Würslin C, Ketelsen D et al.* Automated volumetric assessment of the Achilles tendon (AVAT) using a 3D T2 weighted SPACE sequence at 3T in healthy and pathologic cases. European Journal of Radiology 2012; 81: 1612 – 1617
52 *Khan KM, Forster BB, Robinson J et al.* Are ultrasound and magnetic resonance imaging of value in assessment of Achilles tendon disorders? A two year prospective study. Br J Sports Med 2003; 37: 149 – 153
53 *Gardin A, Bruno J, Movin T et al.* Magnetic resonance signal, rather than tendon volume, correlates to pain and functional impairment in chronic Achilles tendinopathy. Acta Radiol 2006; 47: 718 – 724
54 *Shalabi A, Kristoffersen-Wiberg M, Papadogiannakis N et al.* Dynamic contrast-enhanced MR imaging and histopathology in chronic achilles tendinosis: A longitudinal MR study of 15 patients. Acta Radiologica 2002; 43: 198 – 206
55 *Brushoj C, Henriksen BM, Albrecht-Beste E et al.* Reproducibility of ultrasound and magnetic resonance imaging measurements of tendon size. Acta Radiol 2006 47: 954 – 959
56 *Bashford GR, Tomsen N, Arya S et al.* Tendinopathy discrimination by use of spatial frequency parameters in ultrasound B-mode images. IEEE Trans Med Imaging 2008; 27: 608 – 615
57 *van Schie HTM, de Vos RJ, de Jonge S et al.* Ultrasonographic tissue characterisation of human Achilles tendons: quantification of tendon structure through a novel non-invasive approach. British Journal of Sports Medicine 2010; 44: 1153 – 1159
58 *De Zordo T, Fink C, Feuchtner GM et al.* Real-Time Sonoelastography Findings in Healthy Achilles Tendons. American Journal of Roentgenology 2009; 193: 134 – 138
59 *Drakonaki EE, Allen GM, Wilson DJ.* Real-time ultrasound elastography of the normal Achilles tendon: reproducibility and pattern description. Clinical Radiology 2009; 64: 1196 – 1202
60 *De Zordo T, Chhem R, Smekal V et al.* Real-Time Sonoelastography: Findings in Patients with Symptomatic Achilles Tendons and Comparison to Healthy Volunteers. Ultraschall in Med 2010; 31: 394 – 400
61 *Sconfienza L, Silvestri E, Cimmino M.* Sonoelastography in the evaluation of painful Achilles tendon in amateur athletes. Clin Exp Rheumatol 2010; 28: 373 – 378
62 *Shin D, Finni T, Ahn S et al.* In vivo estimation and repeatability of force-length relationship and stiffness of the human achilles tendon using phase contrast MRI. J Magn Reson Imaging 2008; 28: 1039 – 1045
63 *Robson MD, Bydder GM.* Clinical ultrashort echo time imaging of bone and other connective tissues. NMR Biomed 2006; 19: 765 – 780
64 *Hayes CW, Parellada JA.* The magic angle effect in musculoskeletal MR imaging. Top Magn Reson Imaging 1996; 8: 51 – 56
65 *Oatridge A, Herlihy A, Thomas RW et al.* Magic Angle Imaging of the Achilles Tendon in Patients with Chronic Tendonopathy. Clinical Radiology 2003; 58: 384 – 388
66 *Oatridge A, Herlihy AH, Thomas RW et al.* Magnetic resonance: magic angle imaging of the Achilles tendon. Lancet 2001; 358: 1610 – 1611
67 *Marshall H, Howarth C, Larkman DJ et al.* Contrast-enhanced magic-angle MR imaging of the Achilles tendon. Am J Roentgenol 2002; 179: 187 – 192
68 *Robson MD, Gatehouse PD, Bydder M et al.* Magnetic resonance: an introduction to ultrashort TE (UTE) imaging. J Comput Assist Tomogr 2003; 27: 825 – 846
69 *Hodgson R, Grainger A, O'Connor P et al.* Imaging of the Achilles tendon in spondyloarthritis: a comparison of ultrasound and conventional, short and ultrashort echo time MRI with and without intravenous contrast. European Radiology 2011; 21: 1144 – 1152
70 *Diaz E, Chung CB, Bae WC et al.* Ultrashort echo time spectroscopic imaging (UTESI): an efficient method for quantifying bound and free water. NMR in Biomedicine 2012; 25: 161 – 168
71 *Du J, Statum S, Znamirowski R et al.* Ultrashort TE T1ρ magic angle imaging. Magnetic Resonance in Medicine 2012; 69: 682 – 687
72 *Grosse U, Syha R, Martirosian P et al.* Ultrashort echo time MR imaging with off-resonance saturation for characterization of pathologically altered Achilles tendons at 3 T. Magnetic Resonance in Medicine 2012, Epub ahead of print
73 *Juras V, Zbyn S, Pressl C et al.* Regional variations of T2* in healthy and pathologic achilles tendon in vivo at 7 Tesla: Preliminary results. Magnetic Resonance in Medicine 2011, Epub ahead of print
74 *Syha R, Martirosian P, Ketelsen D et al.* Magnetization Transfer in Human Achilles Tendon Assessed by a 3D Ultrashort Echo Time Sequence: Quantitative Examinations in Healthy Volunteers at 3T. Fortschr Röntgenstr 2011; 183: 1043 – 1050
75 *Wright P, Jellus V, McGonagle D et al.* Comparison of two ultrashort echo time sequences for the quantification of T1 within phantom and human Achilles tendon at 3 T. Magnetic Resonance in Medicine 2012; 68: 1279 – 1284
76 *Wang K, Yu H, Brittain JH et al.* k-space water-fat decomposition with T2* estimation and multifrequency fat spectrum modeling for ultra-

short echo time imaging. Journal of Magnetic Resonance Imaging 2010; 31: 1027 – 1034
77 *Du J*, *Carl M*, *Diaz E et al.* Ultrashort TE T1rho (UTE T1rho) imaging of the Achilles tendon and meniscus. Magnetic Resonance in Medicine 2010; 64: 834 – 842
78 *Juras V*, *Welsch G*, *Bär P et al.* Comparison of 3T and 7T MRI clinical sequences for ankle imaging. European Journal of Radiology 2012; 81: 1846 – 1850
79 *Juras V*, *Apprich S*, *Pressl C et al.* Histological correlation of 7T multiparametric MRI performed in ex-vivo Achilles tendon. European Journal of Radiology 2011, Epub ahead of print
80 *Juras V*, *Zbýň Š*, *Pressl C et al.* Sodium MR Imaging of Achilles Tendinopathy at 7 T: Preliminary Results. Radiology 2012; 262: 199 – 205